Available online at www.sciencedirect.com
SCIENCE DIRECT®
ELSEVIER Computers and Mathematics with Applications 48 (2004) 1121–1133
An International Journal
computers & mathematics
with applications
www.elsevier.com/locate/camwa

# The Laplacian Eigenvalues of a Polygon

P. GRINFELD AND G. STRANG
Department of Mathematics, MIT
Cambridge, MA 02139, U.S.A.
pg@mit.edu
gs@math.mit.edu

**Abstract**—"The difficulties are almost always at the boundary." That statement applies to the solution of partial differential equations (with a given boundary) and also to shape optimization (with an unknown boundary). These problems require two decisions, closely related but not identical:

1. How to discretize the boundary conditions.
2. How to discretize the boundary itself.

That second problem is the one we discuss here. The region $\Omega$ is frequently replaced by a polygon or polyhedron. The approximate boundary $\partial\Omega_N$ may be only a linear interpolation of the true boundary $\partial\Omega$. A perturbation theory that applies to smooth changes of domain is often less successful for a polygon. This paper concentrates on a model problem—the simplest we could find—and we look at *eigenvalues of the Laplacian*.

The boundary $\partial\Omega$ will be the unit circle. The approximate boundary $\partial\Omega_N$ is the regular inscribed polygon with $N$ equal sides. It seems impossible that the eigenvalues of regular polygons have not been intensively studied, but we have not yet located an authoritative reference. The problem will be approached numerically from three directions, without attempting a general theory. Those directions are:

1. Finite-element discretizations of the polygons $\Omega_N$.
2. A Taylor series based on piecewise smooth perturbations of the circle.
3. A series expansion of the eigenvalues in powers of $1/N$.

The second author particularly wishes that we could have consulted George Fix about this problem. His Harvard thesis demonstrated the tremendous improvement that "singular elements" can bring to the finite-element method (particularly when $\Omega$ has a reentrant corner, or even a crack). His numerical experiments in [1] came at the beginning of a long and successful career in applied mathematics. We only wish it had been longer. 

**Keywords**—Laplace eigenvalues, Polygons, Finite elements, Boundary perturbations, Moving boundary derivative.

## INTRODUCTION

Problems with moving interfaces arise in an unexpected variety of situations. We present a problem where moving interfaces provide a key insight in a surprising and welcome fashion: we show how to estimate the spectrum of a regular polygon, with minimal computing power. Only a square and three special triangles have eigenvalues that we know in closed form. The gist of what we are proposing is simple: we deform a circle into a polygon and "track" the evolution of the spectrum. Our technique applies equally well to domains that are slight deformations of shapes

0898-1221/04/$ - see front matter  Typeset by AMS-TEX
doi:10.1016/j.camwa.2004.10.010

with established spectra. Such domains include ellipses with low eccentricity, spheres with dents, and rectangles with round corners. Of course, there are other methods (like finite elements!) that can handle such domains.

The finite-element method [1] is particularly adept at computing the Laplacian eigenvalues of reasonably arbitrary domains. And we would advocate the use of numerical methods whenever possible. Our methodology can in many cases offer significant advantages:

1. When the interface has a high frequency perturbation like $r(\alpha) = 1 + \varepsilon \cos(10^6 \alpha)$, the FEM will require a very high tessellation level near the boundary leading to a large (and potentially ill-conditioned) linear algebra problem. A polygon with many sides represents a perturbation of this sort. Our approach is less sensitive to the complexity of the perturbation than other numerical methods.
2. Our methodology can be effectively combined with numerical methods applied to a nearby problem. The spectrum of an ellipse can be computed numerically and the perturbed spectrum can be computed using our technique.
3. Higher eigenvalues usually require very high tessellation levels to be computed accurately. The accuracy of our technique scales like $O(\lambda)$ compared to $O(\lambda^3)$ for finite elements.

We mention another application to PDEs. The original domain is usually replaced with an approximate one (often a polygon) and the remaining part is thrown away. When finite elements with straight edges are used, the original domain is replaced by a polygon! In level set methods, the boundary of the domain is obscured altogether by the characteristic size of the regular quadratic mesh. It is of key importance to know how large the error can be. This problem has been addressed for Poisson's equation, [2], but the eigenvalue problem seems to have been left behind.

The problems of perturbed spectra arise frequently in physics. In the 1960s, Migdal [3] studied the spectrum of an electron trapped in an ellipsoidal cavity. Migdal found the first-order correction to the spectrum by stretching the Cartesian coordinate system in such a way that the ellipsoid was transformed into a sphere. In the new coordinate system, the Laplacian has a small correction term. In other words, the perturbation is "transferred" from the boundary shape to the operator, and classical perturbation theory can be successfully applied. Migdal's approach can be very useful in finding corrections for spherical systems with ellipsoidal perturbations. The transformation of the circle to a polygon is a more complicated perturbation and requires a more robust technique.

A very promising way to compute eigenvalues of a polygon is suggested in a preprint by Betcke and Trefethen [4], stabilizing the method in the well-known paper of Fox, Henrici and Moler [5].

## FINITE-ELEMENT ESTIMATES

There are three fundamental difficulties in achieving high accuracy with finite elements.

1. Accurate estimates require fine meshes. If the mesh has $P$ nodes, the continuous eigenvalue problem is converted into a $P \times P$ problem which can be sparsely represented by $O(P)$ bytes. The conventional eigenvalue solvers perform an inversion with a shift which requires $O(P^2)$ bytes. A mesh with $10^5$ nodes will challenge our RAM reserves of 1 gigabyte.

   The fine mesh requirement is particularly stringent for polygons with many sides, since a greater density of nodes is necessary near the boundary. Figure 1 shows a typical mesh [6] for a regular polygon with 128 sides.
2. The finite-element errors grow as $O(\lambda^3)$. This becomes a problem rather quickly as the fifth radial eigenvalue on the circle is about $\lambda_5 = 223$.
3. It is difficult to employ Richardson extrapolation—a standard tool in series acceleration—for two reasons:
   (i) The error in estimates for larger eigenvalues, $\lambda > 100$, exceeds the $O(1)$ spacing between the consecutive eigenvalues. For the unit square, the eigenvalues are

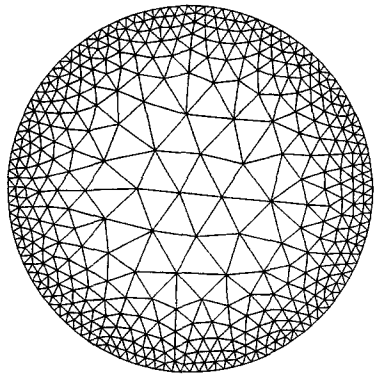

Figure 1. A typical mesh for a 128-sided nearly circular polygon [6].

$\pi^2(n^2+m^2) = \pi^2 r^2$. They have roughly the same distribution as points with integer coordinates in $2D$. No eigenvalues with $m \neq n$ are simple; they are at least double from the pairs $(m,n)$ and $(n,m)$.

(ii) Eigenvalue crossing occurs for subsequent mesh refinements, as it does for

$$A(t) = \begin{bmatrix} 2+t & 0 \\ 0 & 4-t \end{bmatrix}.$$

The eigenvalues $\lambda_1(t)$ and $\lambda_2(t)$ change differentiably with $t$ if defined according to

$$\begin{aligned} \lambda_1(t) &= 2+t, \\ \lambda_2(t) &= 4-t. \end{aligned} \tag{1}$$

Then $\lambda_1(t)$ and $\lambda_2(t)$ are seen to "cross" at $t=1$. If the index is chosen according to the relative magnitude

$$\begin{aligned} \lambda_1(t) &= \min(2+t, 4-t), \\ \lambda_2(t) &= \max(2+t, 4-t), \end{aligned} \tag{2}$$

then the dependence on $t$ is no longer differentiable and the evolution is more difficult to track.

## Richardson Extrapolation

Suppose that the limit of a sequence $a^{(k)}$ is $A_0$ and the convergence is quadratic: $a^{(k)} = A_0 + A_1 k^{-2} + O(k^{-3})$. Then $a^{(2k)} = A_0 + (1/4)A_1 k^{-2} + O(k^{-3})$. Richardson extrapolation forms a new series $b^{(k)} = (1/3)(4a^{(2k)} - a^{(k)})$. The effect is the cancellation of the quadratic terms, $b^{(k)} = \mathcal{R}_2 a^{(k)} = A_0 + O(k^{-3})$. We can expect that $b^{(k)}$ will converge more rapidly than $a^{(k)}$. The new $b^{(k)}$ series can be accelerated further by: $c^{(k)} = \mathcal{R}_3 b^{(k)} = (1/7)(8b^{(2k)} - b^{(k)})$. The two steps, $\mathcal{R}_2$ and $\mathcal{R}_3$, may be combined into a single extrapolation $\mathcal{R}_{2,3}$,

$$\begin{aligned} c^{(k)} &= \frac{1}{7}\left(8b^{(2k)} - b^{(k)}\right) \\ &= \frac{1}{7}\left(8 \times \frac{1}{3}\left(4a^{(4k)} - a^{(2k)}\right) - \frac{1}{3}\left(4a^{(2k)} - a^{(k)}\right)\right) \\ &= \frac{1}{21}\left(32a^{(4k)} - 12a^{(2k)} + a^{(k)}\right). \end{aligned}$$

These $\mathcal{R}_{2,3}$ coefficients $32/21$, $-12/21$, and $1/21$ are the convolution of $4/3$, $-1/3$ from $\mathcal{R}_2$ and $8/7$, $-1/7$ from $\mathcal{R}_3$.

Richardson extrapolation can be used with finite elements. With each refinement the characteristic mesh size $h$ is cut in half. The corresponding eigenvalue estimate $\lambda_h$ is a function of $h$. For linear elements the order of convergence is $h^2$ and $\mathcal{R}_2$ produces a sequence that should converge at least as fast as $h^3$. In reality it converges as $h^4$. We can therefore use $\mathcal{R}_4$ to accelerate the convergence further. For quadratic elements on the same mesh (irregular but reasonable), the leading order in error is $h^4$ and the productive accelerations are $\mathcal{R}_4$, $\mathcal{R}_6$, and $\mathcal{R}_8$.

### Considering a Single Slice

The symmetries offered by regular polygons overcome the obstacles to Richardson extrapolation described above. The trick (suggested by Persson) works for all simple eigenvalues and radially symmetric eigenfunctions. We replace the original polygon by a single slice with Neumann conditions (zero normal derivatives) along the sides. The original radial eigenfunctions are symmetric with respect to rotation by $2\pi/N$ and reflection about the sides of any slice. Therefore, they satisfy zero Neumann conditions and our new problem ought to pick them out. Figure 2 shows a slice of a 16-sided polygon and a typical eigenfunction with Neumann conditions on the sides.

The new PDE also picks up spurious solutions on the slice that cannot be extended to an eigenfunction on the polygon. An example of such a solution can be seen on Figure 3. If two such triangles are arranged side by side, the combined solution will not be continuous.

For eigenvalues $\lambda < 10^4$, there are only a few spurious solutions and we can simply exclude them. An alternative is to replace Neumann conditions with periodic conditions, but this requires a highly regular mesh: the node pattern along each side must be the same. Also, periodic conditions lead to more complicated code. We decided to employ Neumann conditions in the numerical experiments described below.

The main effect of using a slice with Neumann conditions is that the eigenvalues are primarily the ones that correspond to radial eigenfunctions allowing Richardson extrapolation.

What order terms should we cancel when we do not know the true eigenvalues? Our plan is to ascertain the order of convergence from the consecutive differences $\lambda^{(k)} - \lambda^{(k+1)}$. If the $\lambda^{(k)}$

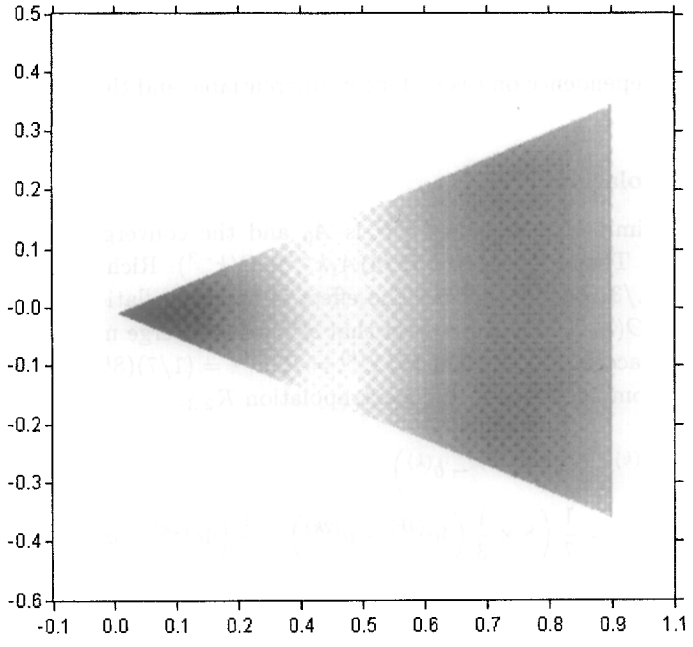


Figure 2. Eigenfunction on a slice of a regular polygon with 16 sides. The brightness indicates the value of the eigenfunction (min = black, max = white).

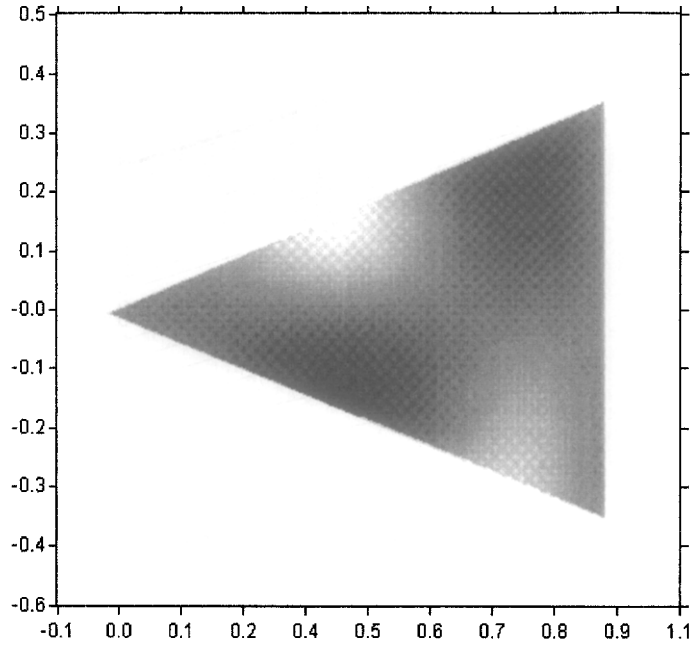


Figure 3. A spurious solution on a single slice of a regular polygon with 16 sides.

converge to $\lambda$ then the differences normally converge to zero at the same rate. We encounter two interesting effects which can be seen in Figure 4: the order of convergence depends on the eigenvalue and the curve for one of the eigenvalues is clearly "out of line". The latter is an example in which eigenvalues cross. The $26^{\text{th}}$ (radial) and the $27^{\text{th}}$ (nonradial) eigenvalue estimates are given by (3). The right choices (indicated in bold) can be made by inspecting the shape of the eigenfunction or by straightening out the difference curves as in Figure 5.

| $h^{-1}$ | 32 | 64 | 128 | 256 |
|---|---|---|---|---|
| $26^{\text{th}}$ estimate | 6058.272 | 6049.884 | 6049.286 | **6048.509** |
| $27^{\text{th}}$ estimate | **6263.288** | **6064.930** | **6049.528** | 6049.247 |

(3)

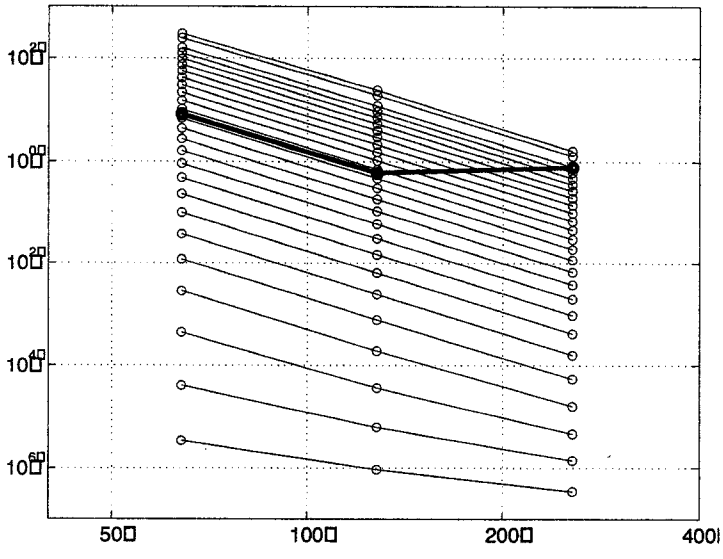


Figure 4. Consecutive differences of eigenvalue estimates. The bold curve is caused by eigenvalue crossing.

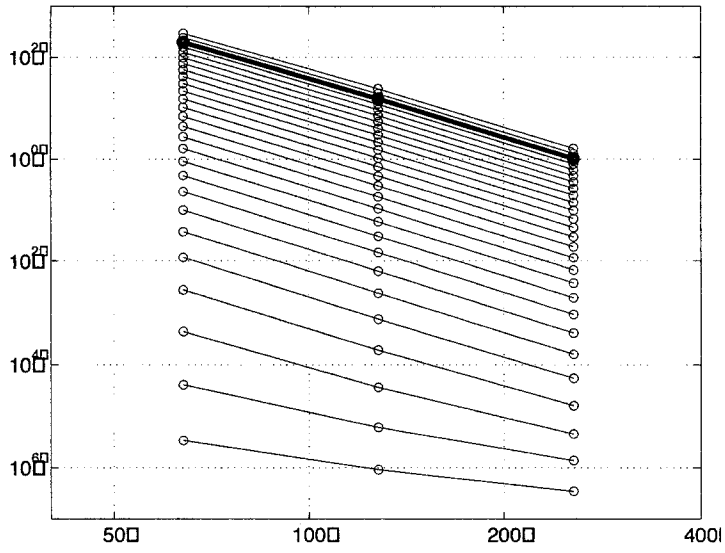


Figure 5. Consecutive differences of eigenvalue estimates. Eigenvalue crossing is removed by renumbering.

For the larger eigenvalues, the order is $O(h^4)$ and we therefore use $\mathcal{R}_4$. For the first few eigenvalues, the order is less clear (Figure 5 shows a change in slope) and Richardson extrapolation needs more care. Fortunately, it is less critical for these eigenvalues since the direct unextrapolated values may be sufficiently accurate. Our eigenvalue estimates are given at the end of the paper.

## THE TAYLOR SERIES APPROACH

In this section we propose an analytical approach to finding the simple eigenvalues on regular polygons with many sides. It can be applied to more general perturbations of a circle and can be used in studying the equilibrium and stability of the so-called *electron bubbles* [8]. The analysis of the second energy variation, which equals the second Taylor term in the vicinity of an equilibrium, reveals a morphological instability of the "$\lambda_2$" (or $2s$) electron bubbles [9].

This Taylor series technique has several attractive features:

1. It requires minimal computing power. (A calculator should be sufficient as long as it can evaluate Bessel functions.)
2. The error in the eigenvalue $\lambda$ grows as $O(\lambda)$ compared to $O(\lambda^3)$ for finite elements. Therefore, we can expect this approach to improve upon finite elements for higher eigenvalues.

Suppose $u(z)$ is a normalized eigenfunction of the Laplace operator on the domain $\Omega$,

$$-\Delta u = \lambda u, \qquad \text{on } \Omega, \tag{4}$$

$$u|_{\partial\Omega} = 0, \qquad \text{on } \partial\Omega, \tag{5}$$

$$\int_\Omega u^2 \, d\Omega = 1, \qquad \text{for normalization.} \tag{6}$$

The eigenvalue $\lambda$ may be expressed as a Rayleigh quotient with unit denominator from (6),

$$\lambda = \int_\Omega |\nabla u|^2 \, d\Omega. \tag{7}$$

Introduce a sufficiently differentiable family of domains $\Omega_t$, such that $\Omega_0$ is the initial circle and $\Omega_1$ is the eventual polygon. We think of $t$ as a time-like parameter; so are $\partial\Omega_t$, $u_t = u(\Omega_t)$ and $\lambda(t)$. In particular, $\lambda(0)$ is an eigenvalue for the circle and $\lambda(1)$ is the corresponding eigenvalue

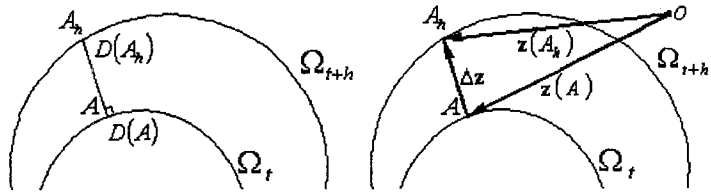


Figure 6. Geometric construction of the $\frac{\delta}{\delta t}$-derivative for $D$ (a scalar or vector) and its application to the radius vector $\mathbf{z}$ (which gives $C$).

for the polygon. The main idea is that $\lambda(1)$ can be approximated as a Taylor series (remember $\Delta t = 1$),

$$\lambda(1) \approx \lambda(0) + \frac{d\lambda(0)}{dt} + \frac{1}{2}\frac{d^2\lambda(0)}{dt^2}. \tag{8}$$

Approximation (8) is valid despite the fact that $\Delta t$ is not small. The derivatives themselves are small since the distance "travelled" by the domains $\Omega_t$ is small.

We will only consider eigenvalues corresponding to radial eigenfunctions. On a polygon, all eigenfunctions depend on the angle—we deal with those that evolved from a radial eigenfunction at $t = 0$ on a circle. The nonradial cases involve multiple eigenvalues and a more complicated perturbation theory. A general perturbation will lift the degeneracy and indicate the correct choice of unperturbed eigenfunctions [7]. Full detail here would obscure the essentials of our findings.

### What a Simple Example Can Teach Us

A simple example demonstrates our idea. Suppose we want to estimate the radial eigenvalues of a circle of radius $1 + \Delta R$. The starting point for our estimate is the radial eigenvalues $\lambda_n$ of the unit circle. A family of uniformly expanding circles $\Omega_t$ is given by

$$r(\alpha, t) = 1 + t\Delta R. \tag{9}$$

Then $\lambda_n(t) = \lambda_n/(1 + t\Delta R)^2$ is represented at $t = 1$ by the Taylor series

$$\lambda_n(1) = \frac{\lambda_n}{(1+\Delta R)^2} = \lambda_n\left(1 - 2\Delta R + 3\Delta R^2 + O\left(\Delta R^3\right)\right). \tag{10}$$

Our technique will calculate the Taylor coefficients (like $-2$ and $3 = (1/2)(6)$) for a more complex evolution of curves. There is every reason to expect that key features will be inherited from this simple example.

First, we assume that $\lambda(t)$ is an analytic function of $t$. If the leading linear term in the Taylor expansion is nonzero, then the difference between the eigenvalue on the circle and the polygon with $N$ sides should be on the order of $O(\Delta R^2) = O(N^{-2})$. Our numerical explorations confirm this. The remaining error $(\lambda_n O(\Delta R^3))$ scales linearly with the eigenvalue. This gives the Taylor series an advantage in computing the larger eigenvalues.

### An Invariant Derivative for Moving Surfaces

The derivatives $\frac{d\lambda}{dt}$ and $\frac{d^2\lambda}{dt^2}$ can be calculated by a repeated application of the so-called $\frac{\delta}{\delta t}$-derivative defined on $\partial\Omega_t$. Consider two nearby times $t$ and $t + h$. Let $A$ be a point on the surface at time $t$. The normal to the surface $\partial\Omega_t$ at point $A$ meets the surface $\partial\Omega_{t+h}$ at point $A_h$. Then, $\frac{\delta D}{\delta t}$ is defined as in Figure 6,

$$\frac{\delta D(A)}{\delta t} = \lim_{h\to 0}\frac{D\left(A_h\right) - D(A)}{h}.$$

This definition applies to vectors $\mathbf{D}$ as well as scalars. The velocity $C = C_t$ of the surface along the normal $\mathbf{N}$ is defined as the $\frac{\delta}{\delta t}$-derivative of the radius vector $\mathbf{z}$,

$$C = \frac{\delta \mathbf{z}}{\delta t} \cdot \mathbf{N}. \tag{11}$$

Since $\frac{\delta \mathbf{z}}{\delta t}$ is parallel to $\mathbf{N}$ (Figure 6), we have $|C| = |\frac{\delta \mathbf{z}}{\delta t}|$.

The surface velocity $C$ is a key quantity, defined over $\partial\Omega_t$. It is analogous to the velocity of a material point and governs the evolution of the surface. However, its profound distinction from the partial derivative of $\mathbf{z}$ is that it does not track material points but rather the surface as an invariant object. If a cylinder is rotating about its axis, $C = 0$ since the picture stays unchanged ($\Omega_{t+h}$ is the same as $\Omega_t$). While $\frac{\partial \mathbf{z}}{\partial t} = 1$ is a straightforward PDE, its surface analog $C = 1$ is equivalent to the Eikonal equation.

We note several relationships for $\frac{\delta}{\delta t}$ needed below. The first two are the critical formulas used to differentiate volume and surface integrals

$$\frac{d}{dt}\int_{\Omega_t} f\, d\Omega = \int_{\Omega_t} \frac{\partial f}{\partial t}\, d\Omega + \int_{\partial\Omega_t} Cf\, dS, \tag{12}$$

and

$$\frac{d}{dt}\int_{\partial\Omega_t} \phi\, dS = \int_{\partial\Omega_t} \frac{\delta \phi}{\delta t}\, dS - \int_{\partial\Omega_t} C\kappa\phi\, dS, \tag{13}$$

where $\kappa$ is (twice) the mean curvature of the surface. The vector or scalar field $f$ is defined in the interior of $\Omega_t$ and is allowed to depend on $t$. The vector or scalar field $\phi$ is defined on $\partial\Omega_t$ and also depends on $t$. It may arise as a restriction of a spatial field or be defined exclusively on the surface, such as the normal vector $\mathbf{N}$. Formula (12) is the moving surface equivalent of the fundamental theorem of calculus, while (13) has no analogue in one-dimensional calculus. For 2D problems, areas replace volumes and contours replace surfaces.

If the field $\phi$ is the surface restriction of a spatial field $f$, we have

$$\frac{\delta \phi}{\delta t} = \frac{\partial f}{\partial t} + C\frac{\partial f}{\partial n}. \tag{14}$$

This formula is analogous to the chain rule of ordinary calculus. Finally, the $\frac{\delta}{\delta t}$-derivative obeys the Leibnitz rule

$$\frac{\delta(\phi\gamma)}{\delta t} = \phi\frac{\delta \gamma}{\delta t} + \frac{\delta \phi}{\delta t}\gamma. \tag{15}$$

**Derivatives of $\lambda(t)$ and $u_t$**

The expression for $\frac{d\lambda}{dt}$ comes from differentiating the Rayleigh quotient (7). It involves $\frac{\partial u}{\partial t}$ on the surface, which can be obtained by applying the $\frac{\delta}{\delta t}$-derivative to the boundary condition (5). The chain rule (14) yields

$$\left.\frac{\partial u}{\partial t}\right|_S = -C\frac{\partial u}{\partial n}. \tag{16}$$

We shall use the fact that the eigenfunction $u$ is orthogonal to its time derivative $\frac{\partial u}{\partial t}$,

$$\int_{\Omega_t} u\frac{\partial u}{\partial t}\, d\Omega = 0. \tag{17}$$

This can be obtained by applying the volume differentiation formula (12) to the normalization condition (6),

$$\int_{\Omega_t} u\frac{\partial u}{\partial t}\, d\Omega + \int_{\partial\Omega_t} Cu^2\, dS = 0.$$

The second term vanishes because of the boundary condition (5).

Now differentiate the Rayleigh quotient (writing $\Omega$ and $\partial\Omega$ for $\Omega_t$ and $\partial\Omega_t$) to obtain $\frac{d\lambda}{dt}$

$$\begin{aligned}
\frac{d\lambda}{dt} &= \frac{d}{dt}\int_\Omega |\nabla u|^2 \, d\Omega, \\
\text{by (12)} &= \int_\Omega \frac{\partial}{\partial t}|\nabla u|^2 \, d\Omega + \int_{\partial\Omega} C\,|\nabla u|^2 \, dS, \\
\text{(Leibnitz rule)} &= 2\int_\Omega \nabla\frac{\partial u}{\partial t}\cdot\nabla u \, d\Omega + \int_{\partial\Omega} C\,|\nabla u|^2 \, dS, \\
\text{(Gauss theorem)} &= 2\int_{\partial\Omega} \frac{\partial u}{\partial t}\frac{\partial u}{\partial n}\, dS + 2\int_\Omega \frac{\partial u}{\partial t}\Delta u \, d\Omega + \int_{\partial\Omega} C\,|\nabla u|^2 \, dS, \\
\text{by (4)} &= 2\int_{\partial\Omega} \frac{\partial u}{\partial t}\frac{\partial u}{\partial n}\, dS + 2\lambda\int_\Omega \frac{\partial u}{\partial t} u \, d\Omega + \int_{\partial\Omega} C\,|\nabla u|^2 \, dS, \\
\text{by (16) and (17)} &= -2\int_{\partial\Omega} C\left(\frac{\partial u}{\partial n}\right)^2 dS + \int_{\partial\Omega} C\,|\nabla u|^2 \, dS.
\end{aligned}$$

Since $u$ vanishes on the boundary, its gradient has only a normal component

$$|\nabla u|^2 = \left(\frac{\partial u}{\partial n}\right)^2$$

and the final expression for $\frac{d\lambda}{dt}$ becomes

$$\frac{d\lambda}{dt} = -\int_{\partial\Omega} C\,|\nabla u|^2 \, dS. \tag{18}$$

This formula applies to general domains at all times $t$. The minus sign shows that if the domain expands, its eigenvalues diminish.

The second derivative is computed by a direct differentiation of (19) and is given by

$$\frac{d^2\lambda}{dt^2} = -\int_{\partial\Omega} \frac{\delta C}{\delta t}|\nabla u|^2 \, dS - 2\int_{\partial\Omega} C\frac{\delta\nabla u}{\delta t}\cdot\nabla u \, dS + \int_{\partial\Omega} C^2\kappa\,|\nabla u|^2 \, dS. \tag{19}$$

It is illustrative to show that expressions (18) and (19) yield $\frac{d\lambda_n}{dt} = -2\lambda_n\Delta R$ and $\frac{d^2\lambda_n}{dt^2} = 6\lambda_n\Delta R^2$ for the expanding circle example. We demonstrate the first identity. The radial eigenfunctions $u_n(r)$ on a unit circle are given by Bessel functions

$$u_n(r) = \frac{1}{\sqrt{\pi}J_1(\rho_n)}J_0(\rho_n r), \qquad \text{with eigenvalue } \lambda_n = \rho_n^2.$$

$J_m$ is a Bessel function of the first kind and $\rho_n$ is the $n^{\text{th}}$ positive root of $J_0(r)$.

It is straightforward to verify that $C = \Delta R$ for the family of expanding circles (9). As expected,

$$\left.\frac{d\lambda_n(t)}{dt}\right|_{t=0} = -\frac{1}{\pi}\rho_n^2\int_0^{2\pi}\Delta R\, d\alpha = -2\rho_n^2\Delta R = -2\lambda_n\Delta R.$$

## A Regular Polygon with $N$ Sides

We now apply equations (18) and (19) to our central problem: the eigenvalues on a regular polygon. In a family of curves that evolve from the circle to the polygon, each point moves along the radius with a speed proportional to the distance that it needs to travel. All points reach the polygon at $t = 1$. With radius $R = 1$ and $N$ sides, we focus on one slice of the circle occupying

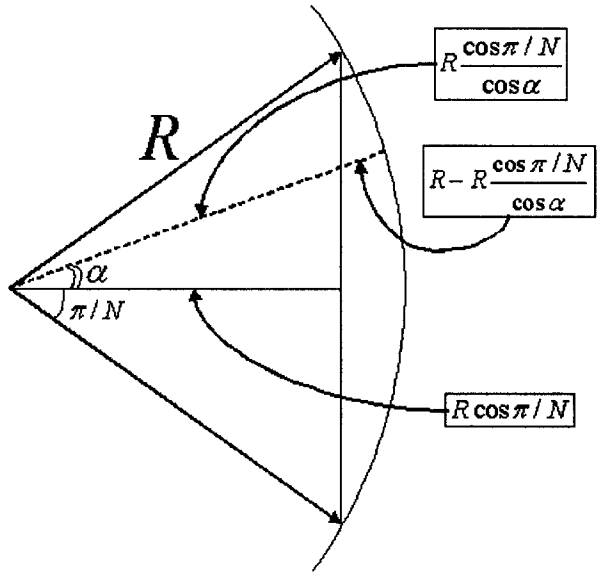


Figure 7. A single slice of an inscribed polygon.

an angle $2\pi/N$ (Figure 7). Center the slice around the $x$-axis and parameterize it with angle $\alpha \in [-\pi/N, \pi/N]$. In polar coordinates the desired family is given by

$$r(\alpha, t) = 1 - t\left(1 - \frac{\cos\pi/N}{\cos\alpha}\right).$$

Figure 7 indicates that the normal velocity of the interface $C^{(N)}$ for this family of curves is given by

$$C^{(N)}\Big|_{t=0} = \frac{\cos\pi/N}{\cos\alpha} - 1 = -(\text{distance traveled}).$$

Its invariant time derivative vanishes at $t = 0$, removing the first term in (19)

$$\frac{\delta C^{(N)}}{\delta t}\bigg|_{t=0} = 0.$$

### The First Taylor Coefficient

To calculate $\frac{d\lambda}{dt}$ for spherically symmetric configurations, equation (18) reduces to

$$\frac{d\lambda}{dt} = -\left(\frac{du}{dr}\right)^2 \int_S C\, dS.$$

The integral is easy to evaluate

$$\frac{d\lambda_n}{dt} = -2\lambda_n\left(\frac{N}{2\pi}\cos\frac{\pi}{N}\ln\frac{1+\sin\pi/N}{1-\sin\pi/N} - 1\right). \tag{20}$$

The first derivative is strictly proportional to $\lambda_n$. The quantity $\int_S C\, dS$ represents the change in area induced by the motion of the interface. For motions that initially conserve area, the linear term $\frac{d\lambda}{dt}$ vanishes.

### The Second Taylor Coefficient

The second Taylor coefficient, although straightforward, is more challenging. We present the final answer and omit the details, which can be found in [7]

$$\left.\frac{d^2\lambda_n}{dt^2}\right|_{t=0} = 4\lambda_n\left(\left|C_0^{(N)}\right|^2 + \sum_{m\neq 0}\left|C_m^{(N)}\right|^2 \frac{\rho_n J_m'(\rho_n)}{J_m(\rho_n)}\right), \tag{21}$$

where $C_m$ is the Fourier coefficient in the decomposition of $C^{(N)}$

$$C^{(N)} = \sum_{m=-\infty}^{\infty} C_m^{(N)} e^{im\theta}. \tag{22}$$

Expression (21) can be easily calculated in MATLAB or in a symbolic package such as Maple. Due to the periodicity in $C^{(N)}$, the coefficient $C_m^{(N)}$ vanishes unless $m$ is a multiple of $N$.

## EXPANSION IN POWERS OF $N$

Suppose that $\lambda_n^{(N)}$ is the $n^{\text{th}}$ simple eigenvalue for an $N$-sided regular polygon. We express $\lambda_n^{(N)}$ as a series in powers of $1/N$

$$\lambda_n^{(N)} = \lambda_n\left(1 + a_{1n}\frac{1}{N} + a_{2n}\left(\frac{1}{N}\right)^2 + \cdots\right), \tag{23}$$

where $\lambda_n$ is the corresponding eigenvalue on the circle.

The $a_{in}$ can be determined from the Taylor series by expanding each term in powers of $1/N$. The first nonzero term is $O(1/N^2)$ and can be determined from the first Taylor term

$$\begin{aligned}\frac{d\lambda_n(0)}{dt} &= -2\lambda_n\left(\frac{N}{2\pi}\cos\frac{\pi}{N}\ln\frac{1+\sin\pi/N}{1-\sin\pi/N} - 1\right)\\ &= \lambda_n\left(\frac{2}{3}\pi^2\frac{1}{N^2} + \frac{2\pi^6}{315}\frac{1}{N^6} + O\left(\frac{1}{N^8}\right)\right).\end{aligned}$$

Therefore, $a_{1n} = 0$ and $a_{2n}$ is independent of $n$,

$$a_{2n} = \frac{2}{3}\pi^2.$$

Figure 8 shows the difference between the first 10 simple eigenvalues on regular $N$-sided polygons and the circle. The slope of $-2$ tells us that convergence is quadratic.

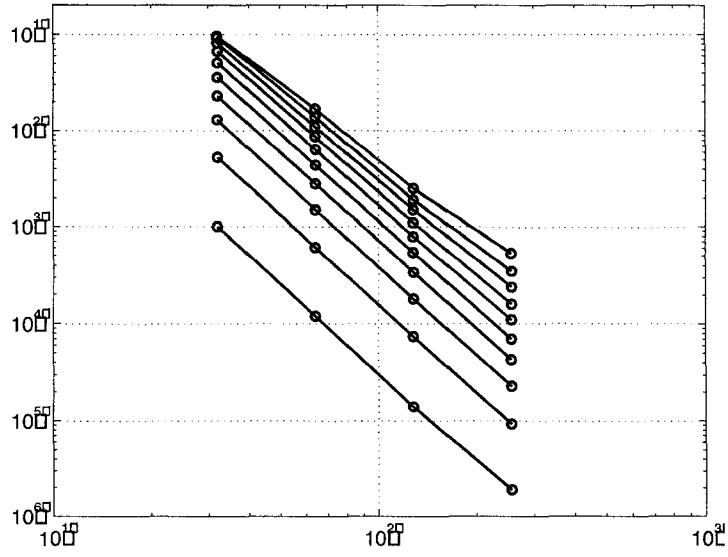

Figure 8. $\lambda_n^{[N]} - \lambda_n$ decreases like $1/N^2$ for the first ten simple eigenvalues ($n = 1$ at the bottom is smallest).

To determine the next term in (23), we computed the difference $\Delta$ between $\lambda_n(1 + (2/3) \cdot (\pi^2/N^2))$ and $\lambda_n^{[N]}$. The slope was $-3$, indicating that the next term is $O(N^{-3})$. Numerically, the average for the quantity

$$\frac{\Delta}{N^3} = \frac{\lambda_n \left(1 + (2/3)\left(\pi^2/128^2\right)\right) - \lambda_n^{[128]}}{128^3}$$

over the first ten eigenvalues equals 5.1570. We can therefore conjecture that

$$a_{3n} = \frac{\pi^3}{6}.$$

It seems very likely that the series (23) has been established by earlier authors!

## RESULTS AND COMPARISON

The finite-element estimates in this section came from these parameters:

1. The regular polygon had $N = 128$ sides.
2. The finite elements were quadratic (six parameters per triangle). For a given amount of RAM, this is better than using linear test and trial functions on a more refined mesh.
3. Richardson extrapolation used meshes that represent 6, 7, and 8 successive refinements of the slice. These meshes contained 2145, 8385, and 33153 nodes and 4096, 16384, and 65536 elements.
4. We employed the Richardson extrapolation $\mathcal{R}_4$ that cancels the $h^4$ terms.

We do not know the true eigenvalues. Therefore we study the difference between the finite-element and Taylor series estimates. That difference is plotted against the eigenvalue itself on a log-log graph in Figure 9 and it is immaterial which of the estimates is used for the $x$-axis. The three curves correspond to the Taylor series estimates with one term ($\lambda_n$), two terms ($\lambda_n + \lambda_n'$), and three terms ($\lambda_n + \lambda_n' + (1/2)\lambda_n''$).

The data is consistent with the following conjecture. For $\lambda < 1000$, the finite-element estimate is closer to the true polygon eigenvalue. Therefore, the difference between the estimates essentially

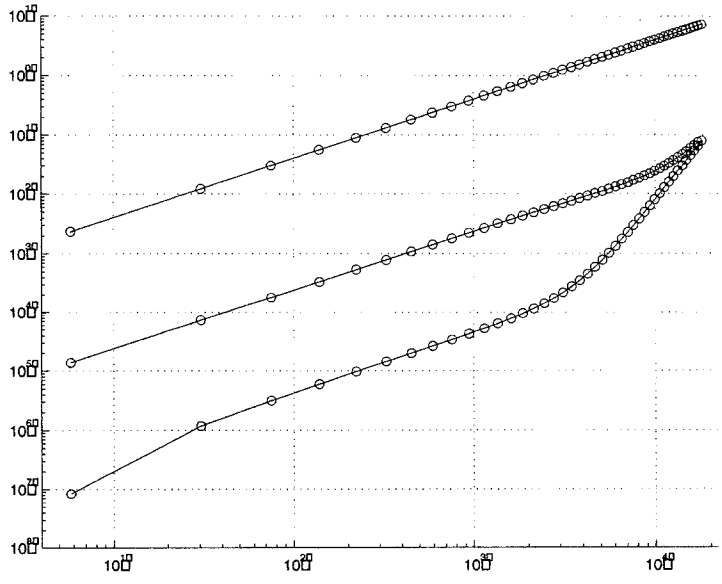

Figure 9. The differences between the FEM and Taylor estimates for $\lambda < 20000$.

represents the error in the Taylor series. Each term in that expansion reduces the error by a factor of 100. The error grows linearly with the eigenvalue. This is precisely what the "expanding circle" example would suggest.

For $\lambda > 1000$ the three-term Taylor series wins over finite elements. The plotted difference is essentially the FE error, which grows as $\lambda^3$. Until roughly $\lambda = 10000$, the finite-element estimate is better than the Taylor series with two terms. This is no longer true for $\lambda > 10000$ and soon the two lowest curves meet, for they both represent the finite-element error.

Table (24) shows our estimates for the first ten simple eigenvalues on the regular 128-sided polygon.

$$\begin{aligned} \lambda_1 &= 5.78552, & \lambda_6 &= 326.69528, \\ \lambda_2 &= 30.48357, & \lambda_7 &= 450.11529, \\ \lambda_3 &= 74.91726, & \lambda_8 &= 593.28245, \\ \lambda_4 &= 139.09646, & \lambda_9 &= 756.19675, \\ \lambda_5 &= 223.02237, & \lambda_{10} &= 938.85822. \end{aligned} \tag{24}$$

## REFERENCES


1. G. Strang and G. Fix, *An Analysis of the Finite Element Method*, Wellesley-Cambridge Press, Wellesley, MA, (1973).
2. G. Strang and A. Berger, The change in solution due to change in domain, In *AMS Symposium on Partial Differential Equations*, Berkeley, pp. 199–206, (1971).
3. A.B. Migdal, *Qualitative Methods in Quantum Theory*, W.A. Benjamin, Reading, MA, (1977).
4. T. Betcke and L.N. Trefethen, Reviving the method of particular solutions, Preprint.
5. L. Fox, P. Henrici and C. Moler, Approximations and bounds for eigenvalues of elliptic operators, *SIAM J. Numer. Analysis* **4**, 89–102, (1967).
6. P.-O. Persson and G. Strang, A simple mesh generator in MATLAB, *SIAM Review* **46**, 329–345, (2004).
7. P. Grinfeld, Numerical solutions of physical problems governed by the principle of minimum energy, Thesis, Department of Mathematics, MIT, (2003).
8. J. Classen, C.-K. Su and H.J. Maris, Observation of exploding electron bubbles in liquid helium, *Phys. Rev. Lett.* **77** (10), 2006, (1996).
9. P. Grinfeld and H. Kojima, Instability of the 2S electron bubbles, *Phys. Rev. Lett.* **91** (10), 9007, (2003).